04

Research and creation of broadband X-ray mirrors with a spectral transmission band coinciding with emission lines and the possibility of filtering

© S.A. Garakhin, I.S. Dubinin, S.Yu. Zuev, V.N. Polkovnikov, N.I. Chkhalo

Institute of Physics of Microstructures, Russian Academy of Sciences,
603087 Nizhny Novgorod, Russia
e-mail: garahins@ipmras.ru

Received April 27, 2022
Revised April 27, 2022
Accepted April 27, 2022

The article considers broadband multilayer X-ray mirrors based on Mo/Be and Mo/Si structures with a transmission band coinciding with the Si $L\alpha$ (13.5 nm) and Sn (13.5 nm) emission lines. The described structures are of great interest for the currently developed liquid source of EUV radiation, since they make it possible to increase the efficiency of the source-X-ray optical system due to the „complete“ capture of emission lines.

Keywords: extreme ultraviolet radiation, emission spectrum, laser spark, multilayer X-ray mirror.

DOI: 10.21883/TP.2022.08.54552.118-22

Introduction

Currently, optical elements such as X-ray mirrors are of great interest. They are used to work with X-ray radiation (collimation, transmission, control of electromagnetic radiation beams). These mirrors are used as reflecting elements for both soft and hard X-rays. They are used in such fields of science as X-ray astronomy, plasma diagnostics, X-ray fluorescence analysis and much more.

X-ray mirrors are a multilayer structure of alternating films of materials with different permittivity values deposited on an ultra-smooth substrate.

The selection of mirror materials and their thicknesses optimized for a specific sub-wavelength range gives a high peak reflection coefficient from such a structure at the selected wavelength. Along with the optical properties of materials, the characteristics of mirrors are influenced by the quality of such a structure, which, as a rule, depends on the conditions of mirror synthesis. If we consider periodic structures, then in this case we are talking about the constancy of the period.

A serious obstacle to the use of periodic mirrors in the extreme ultraviolet (EUV) region is their limited spectral range. The spectral width at half the height for a periodic mirror often covers only a small part of the output signal of some EUV sources. This problem is solved by using broadband mirrors [1–3]. However, an increase in bandwidth is inevitably associated with a decrease in the maximum peak reflectivity. In the case where maximum peak reflectivity is not required, it is reasonable to use broadband mirrors.

Similar structures are often used in EUV metrology, astronomy and microscopy. The use of such mirrors in combination with a broadband plasma source can provide higher system efficiency and collect more radiation from the source. Thus, the use of aperiodic structures makes it possible to satisfy other conditions necessary as part of a specific task. For example, expanding the angular [4,5] or spectral [6,7] operating range, increasing the integral reflection coefficient [8], working as a polarizer, filter [9,10] or controlling pulses of electromagnetic radiation of subfemtosecond duration [11,12]. In each of the specific cases, it is necessary to impose additional conditions when optimizing the structure of such mirrors.

1. Method of optimization of the periodic mirror

The engineering of broadband mirrors that satisfy a predetermined criterion is included in the class of optimization problems and is most often solved using a genetic algorithm. At the first stage, the objective function F_{gf} is determined. For various mirrors, target functions of a special kind were set, highlighting the desired area by wavelengths $R(\lambda)$ or the corners of $R(\theta)$. Next, the norm of the difference between the reflection coefficient and F_{gf} is introduced— the estimated functional F, calculated in the domain of F_{gf} definition and representing a function of N variables (in this case, the thickness of the layers of the structure were used as fitting parameters). Then the optimal structure of the layers is found by minimizing the functional [6,7].

$$F = \int [R(\lambda) - F_{gf}]^2 d\lambda.$$

The initial structures for the first step are periodic mirrors with a maximum reflection at a wavelength corresponding to the maximum of the emission line. The optimization process was carried out with the specified real roughness.

Table 1. Calculated characteristics of optimized stack mirrors Mo/Be

Characteristics	Periodic mirror	Stack 1(first optimized Mo/Be structure)	Stack 2 (second optimized Mo/Be structure)
R_{peak}, %	68	45.9	34.5
$R_{integral}$, Å	5.48	7.02	7.08
FWHM, Å	6.19	17.31	21.09

In any optimization problem there is a problem of possible falling into local minima. Therefore, it is necessary to run optimization repeatedly, and then choose the best structure. But even with this, the achievement of a global minimum is not guaranteed, however, a solution in a local minimum close to the global minimum is sufficient for practice. At the same time, the optimization procedure must be run repeatedly to select the most suitable solution. The optimization technique is described in detail in [13,14].

2. Stock mirrors Mo/Be and Mo/Si with spectral bandwidth coinciding with the emission lines of tin and silicon

Currently, a radiation source at a wavelength of 13.5 nm [15] is being developed on the basis of the tin emission line. The task of maximum collection of such radiation is urgent. It is required to calculate and synthesize an X-ray mirror that would capture the maximum radiation from the source.

According to the method described above, stock mirrors were calculated based on the Mo/Be structure, which has

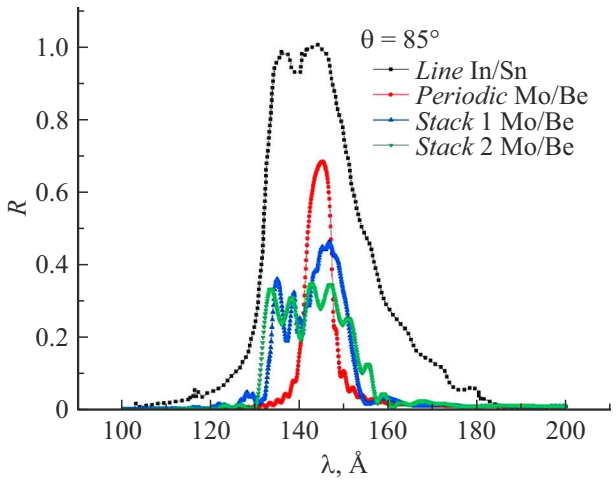

Figure 1. In/Sn emission line, *Stack 1* and *Stack 2* — the best optimized Mo/Be structures consisting of three periodic mirrors that provide the maximum integral reflection coefficient. The *Periodic* Mo/Be dependency is added for comparison with the periodic case.

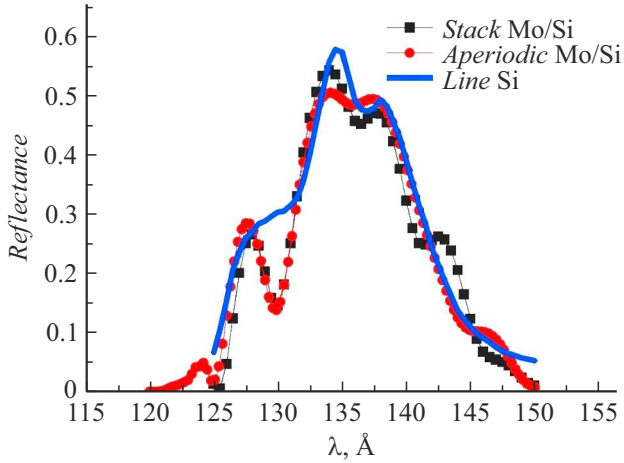

Figure 2. $R(\lambda)$ stack and aperiodic mirrors, repeating the profile of the emission line Si (13.5 nm).

already demonstrated its promise for creating broadband stack mirrors [16]. The shape of the emission line was set as the objective function. Optimization was carried out in the program Multifitting [17]. Optimized mirrors consist of three periodic structures and provide the maximum integral reflection coefficient. The two best variants of the structure, as well as a comparison of their parameters with the periodic case, are presented in Table 1.

The integral reflectivity for stock mirrors is approximately 30% higher than that of periodic mirrors (Fig. 1). Considering the capture of the Sn emission line, this will give an increase in the final intensity of about 6%.

Due to the fact that there is no direct access to the indium-tin-based source at the moment, the methodology for testing the creation of a stack mirror was conducted by us for a source based on an X-ray tube on the Si 13.5 nm line. Thus, the task was to calculate and synthesize a mirror whose coefficient repeats the shape of the silicon emission line with a maximum of 13.5 nm. Due to the special technological limitations that are imposed on working with Ve (special laboratory, harmfulness), testing of the methodology was carried out on the classical structure of Mo/Si.

The optimization results are shown in Fig. 2. Both stack and aperiodic design were considered. The resulting

Table 2. Parameters of the Mo/Si stack structure. Stack numbering from the substrate

Stack	1	2	3
N (number of layers)	11	9	11
Mo	2.9 nm	3.4 nm	3.5 nm
Si	3.7 nm	3.4 nm	3.7 nm

reflection coefficient repeats the shape of the Si emission line fairly accurately, while the structure of the stack mirror is much simpler — there are only three periodic mirrors (Table 2 — numbering from the substrate).

3. Synthesis of the Mo/Si stack mirror. Calibration of deposition parameters

Samples of multilayer Mo/Si mirrors were made by magnetron sputtering in an argon atmosphere at a pressure of $1 \cdot 10^{-3}$ Tor; silicon wafers for the microelectronic industry [18] were used as substrates. A detailed description of the technological installation is contained in [19]. As per the low-angle X-ray diffraction data, observed with use of four-crystal high-resolution diffractometer PANalitycal X'Pert Pro (wavelength is 0.154 nm), the inverse problem is solved, resulting in determination of synthesis parameters of thickness of layers, containing in the required broadband mirror, with high accuracy. At the working wavelength, the mirrors were studied using a reflectometer developed at the IFM RAS, in which the monochromatization of radiation is carried out using a high-resolution Cherni-Turner spectrometer with a flat diffraction grating, two spherical collimating mirrors and a laser-plasma radiation source [20].

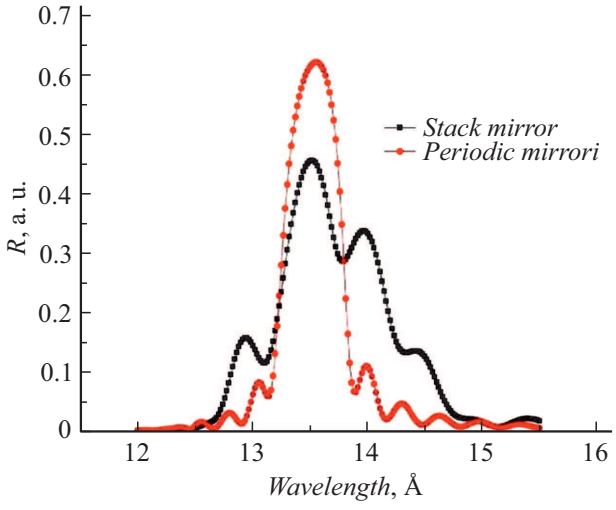

Figure 3. Comparison of measured reflection coefficients for periodic and stack Mo/Si structures.

To speed up the calibration process, Mo/Si structures were sprayed, which consist of two, rather than three periodic structures, with a fixed thickness of one material.

This approach to the calibration of layer thicknesses allows you to significantly reduce the time of work on a specific mirror, as it allows you to calibrate three thicknesses in one deposition instead of two.

4. Experimental results

Fig. 3 shows the resulting reflection of a stack mirror and a comparison with a periodic mirror. The gain in the integral reflection coefficient, which was about 24%, is close to theoretical calculations.

Fig. 4, *a* shows the Si emission line normalized by unit and the dependence of the mirror reflection coefficient for periodic and stack cases. The resulting reflection hitting the detector will be a convolution of these two functions. Fig. 4, *b*, the emission line is normalized to the maximum of the reflection coefficient of the broadband mirror to demonstrate the correspondence of their profiles.

The gain on the signal for the stack mirror compared to the periodic mirror was approximately 6%. Thus, the use of stock mirrors is appropriate for single-mirror schemes. However, for multi-mirror schemes, for example, for the case of X-ray lithography, where up to 9–12 mirrors can be used, such stack mirrors will not give advantages, so in this case only a very narrow spectral range works (Fig. 5).

5. Optimization of the design of stack mirrors with the ability to filter closely spaced spectral lines

In sec. 5 shows how the optimization conditions for an aperiodic (stack) mirror change significantly when considering another field of application. For a number of tasks, certain conditions are required for the filtering properties of X-ray mirrors [21]. So, there is a problem of isolating the maximum signal at a certain wavelength, for example, the Fe-XV (28.4 nm) line in the solar plasma [22]. A magnesium-based mirror copes well with this task, it shows a higher reflection coefficient at this wavelength compared to other pairs of materials (Fig. 6).

The problem is that, firstly, there is a partial capture of the neighboring line 30.4 nm — a parasitic signal that needs to be suppressed, so it is necessary to develop a mirror that will act as a filter, namely, to get maximum information from the useful signal and suppress the parasitic signal. Secondly, a significant disadvantage of magnesium-based mirrors is the temporary instability of their reflective characteristics. Magnesium — is an active material subject to oxidation when stored in room conditions. And if in a massive sample the oxidation processes can be stopped in a thin near-surface layer, then in thin-film systems it is extremely difficult to contain them. Therefore, the most

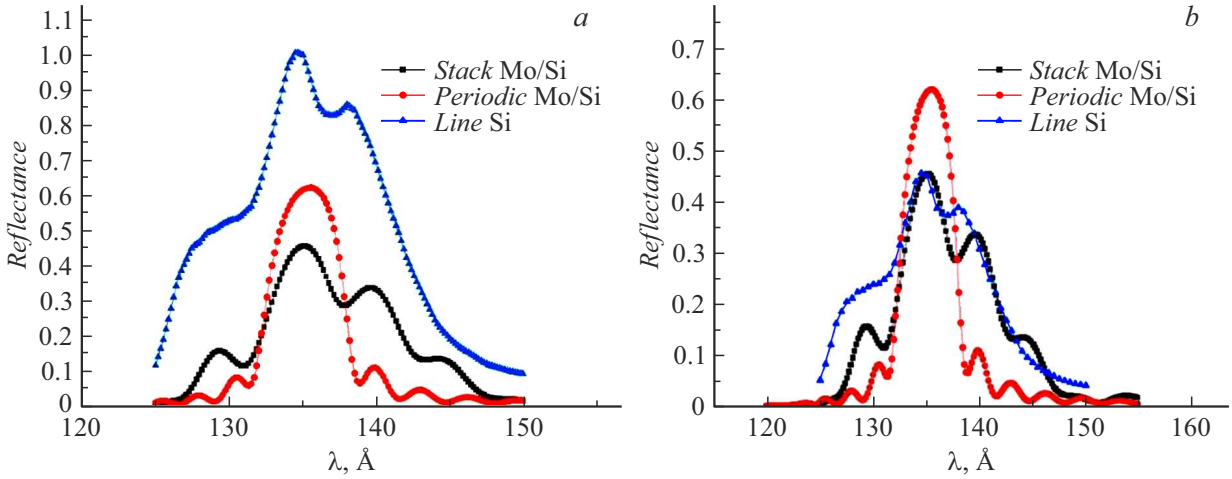

Figure 4. Calculation of the capture efficiency of the emission line Si. *a* — calculation for the unit-normalized case, *b* — shows how the profile of the reflection coefficient corresponds to the profile of the emission line Si.

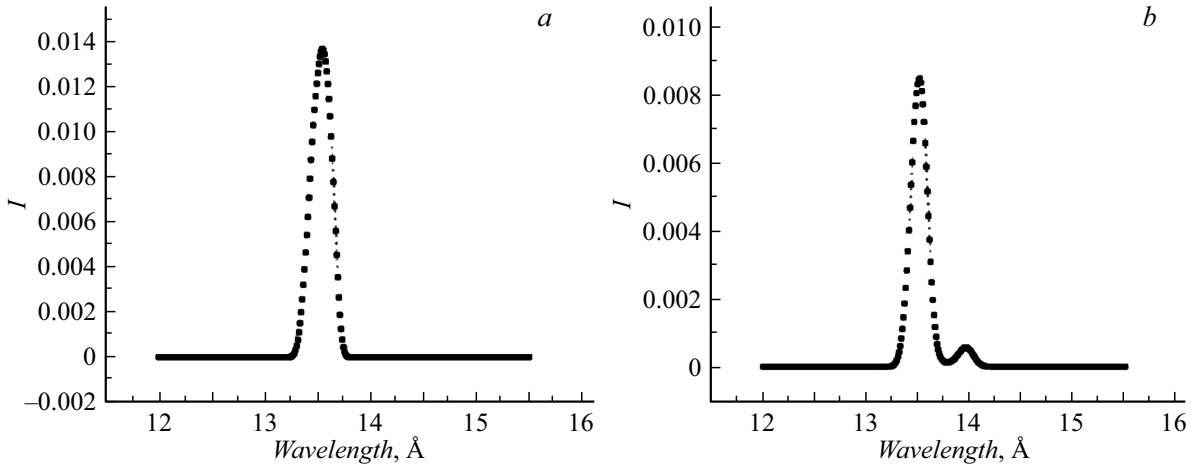

Figure 5. The resulting reflection coefficient for the nine mirror system. *a* — using periodic mirrors in a nine-mirror scheme, *b* — using stack mirrors in a nine-mirror scheme.

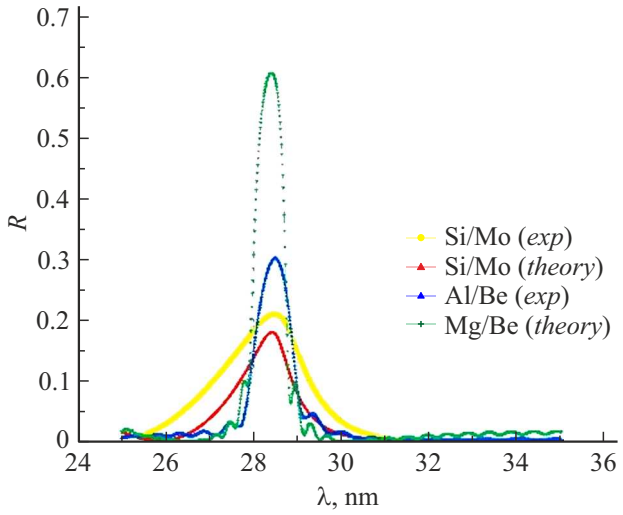

Figure 6. Comparison of reflection coefficients of various periodic structures for the spectral region near 28.4 nm.

important problem of magnesium multilayer structures is the development of protective coatings.

In the study [23], the authors proposed a method for optimizing filtering stack X-ray mirrors, which allows minimizing the contribution of noise from nearby spectral lines to the measured useful signal. The applied method consists in adding a suitable layer covering the multilayer structure, which minimally affects the peak reflectivity, while suppressing unwanted radiation from relatively close lines. It will be shown below that at the same time it can also act as a protective layer if it is optimized on the basis of a time-stable multilayer structure.

The main idea of the method is to consider the propagation of incident and reflected standing waves in the structure from the target and parasitic lines (Fig. 7).

Depending on the task, the covering layer can be implemented using a multi-layer stack or aperiodic structure (up to one layer) of various materials, for example, to obtain additional mechanical or optical properties, such as

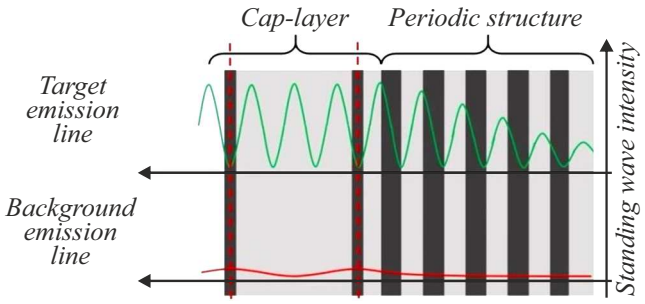

Figure 7. The principle of developing a filter layer for a signal from a parasitic emission line [21].

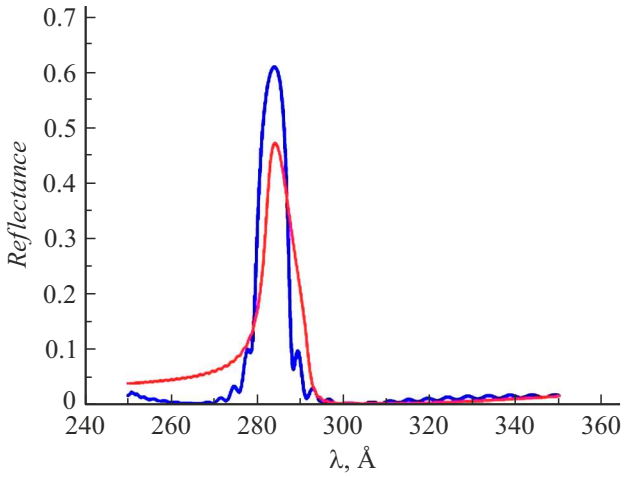

Figure 8. Mg/Be filter mirror with protective filter coating (red curve (in online version)) and periodic structure (blue curve (in online version)).

temporary stability for Mg/Be structures that, in the absence of a protective coating, oxidize over time. Optimization was performed in the program IMD [24]. The results are shown in Fig. 8.

Filtration of the emission line 30.4 nm is carried out at the level of $10^{-4}-10^{-5}$. At the same time, the reflection coefficient at the target wavelength of 28.4 nm fell not so significantly.

Conclusion

Aperiodic and stack multilayer mirrors make it possible to significantly expand the scope of application of classical periodic mirrors. Depending on the task, the optimization technique of such structures may differ significantly.

Based on the study results:

1) Mo/Be stack structures optimized for the maximum of the integral reflection coefficient are calculated to capture radiation from a source based on Sn. The gain in the integral reflection coefficient for stack mirrors compared to periodic mirrors was approximately 30%. With the capture of the emission line, this will give an increase of about 6%.

2) Due to the lack of access to the Sn source, Mo/Si stack and aperiodic mirrors for capturing the emission line Si were calculated to refine the technique. Stack and periodic mirrors were made that capture the radiation from the Si line as much as possible. The gain in the integral reflection coefficient for the stack mirror compared to the periodic one was 24%, which is slightly lower than the theoretically calculated one. The gain on the signal was about 5–6%. For the case of the Sn source and the Mo/Be mirror, the same gain on the signal is expected.

3) A general conclusion is made on the relevance of broadband mirrors for single- and multi-mirror circuits. It is shown that for lithographic installations containing up to 9–12 mirrors, stack mirrors are impractical to use. However, broadband mirrors provide a win for single-mirror systems.

4) To demonstrate a strong difference in the optimization technique depending on the task and application of stack mirrors, the principle of structures capable of not only reflecting the target wavelength, but also suppressing background radiation from nearby lines is described. Such stack mirrors with a specially optimized cover layer can serve as effective filter elements.

Funding

The study was supported by RFBR grant 20-02-00708 and State Assignment 0030-2021-0022.

Conflict of interest

The authors declare that they have no conflict of interest.

References

[1] E.A. Vishnyakov, A.O. Kolesnikov, A.S. Pirozhkov, E.N. Ragozin, A.N. Shatokhin. *Aperiodicheskiye elementy v optike myagkogo rentgenovskogo diapazona* (Fizmatlit, M., 2018), p. 136. (in Russian).
[2] A.L. Aquila, F. Salmassi, F. Dollar, Y. Liu, E.M. Gullikson. Opt. Express, **14** (21), 10073 (2006).
[3] K. Tamura, H. Kunieda, Y. Miyata, T. Okajima, T. Miyazawa, A. Furuzawa, H. Awaki, Y. Haba, K. Ishibashi, M. Ishida, Y. Maeda, H. Mori, Y. Tawara, S. Yamauchi, K. Uesugi, Y. Suzuki. J. Astronom. Telescop., Instruments, Systems, **4** (1), 011209 (2018).
[4] A.E. Yakshin, I.V. Kozhevnikov, E. Zoethout, E. Louis, F. Bijkerk. Opt. Express, **18** (7), 6957 (2010).
[5] I.V. Kozhevnikov, A.E. Yakshin, F. Bijkerk. Opt. Express, **23** (7), 9276 (2015).
[6] N.N. Kolachevsky, A.S. Pirozhkov, E.N. Ragozin. Kvant. elektron., **30** (5), 428 (2000). (in Russian).
[7] E.A. Vishnyakov, F.F. Kamenets, V.V. Kondratenko, M.S. Luginin, A.V. Panchenko, Yu.P. Pershin, A.S. Pirozhkov, E.N. Ragozin. Kvant. elektron., **42** (2), 143 (2012). (in Russian).
[8] P. Van Loevezijn, R. Schlatmann, J. Verhoeven, B.A. Van Tiggelen, E.M. Gullikson. Appl. Opt., **35** (19), 3614 (1996).

[9] Z. Wang, H. Wang, J. Zhu, F. Wang, Z. Gu, L. Chen, A.G. Michette, A.K. Powell, S.J. Pfauntsch, F. Schafers. J. Appl. Phys., **99** (5), 056108 (2006).
[10] Z. Wang, H. Wang, J. Zhu, Y. Xu, S. Zhang, C. Li, F. Wang, Z. Zhang, Y. Wu, X. Cheng, L. Chen, A.G. Michette, A.K. Powell, S.J. Pfauntsch, F. Schafers, A. Gaupp, M. MacDonald. Appl. Phys. Lett., **89** (24), 241120 (2007).
[11] I.L. Beigman, A.S. Pirozhkov, E.N. Ragozin. Pisma v ZhTF, **7** (3), 167 (2001). (in Russian).
[12] I.L. Beigman, A.S. Pirozhkov, E.N. Ragozin. J. Opt. A: Pure Appl. Opt., **4**, 433 (2002).
[13] T. Kuhlmann, S. Yulin, T. Feigl, N. Kaiser, H. Bernitzki, H. Lauth. Proc. SPIE, **4688**, 509 (2002).
[14] M.M. Barysheva, S.A. Parakhin, S.Yu. Zuev, V.N. Polkovnikov, N.N. Salashchenko, M.V. Svechnikov, R.M. Smertin, N.I. Chkhalo, E. Meltchakov. ZhTF **89** (11), 1763 (2019) (in Russian). DOI: 10.21883/TP.2022.08.54552.118-22
[15] D.B. Abramenko, P.S. Antsiferov, D.I. Astakhov, A.Yu. Vinokhodov, I.Yu. Vichev, R.R. Gayazov, A.S. Grushin, L.A. Dorokhin, V.V. Ivanov, D.A. Kim, K.N. Koshelev, P.V. Krainov, M.S. Krivokorytov, V.M. Krivtsun, B.V. Lakatosh, A.A. Lash, V.V. Medvedev, A.N. Ryabtsev, Yu.V. Sidelnikov, E.P. Snegirev, A.D. Solomyannaya, M.V. Spiridonov, I.P. Tsygvintsev, O.F. Yakushev, A.A. Yakushkin. UFN, **189** (3), 330 (2019). (in Russian).
[16] M.M. Barysheva, S.A. Garakhin, A.O. Kolesnikov, A.S. Pirozhkov, V.N. Polkovnikov, E.N. Ragozin, A.N. Shatokhin, R.M. Smertin, M.V. Svechnikov, E.A. Vishnyakov. Opt. Mater. Express, **11**, 3038 (2021). DOI: 10.1364/OME.434506
[17] M. Svechnikov. J. Appl. Crystallog., **53** (1), 244 (2020). https://doi.org/10.1107/S160057671901584X
[18] M.M. Barysheva, Yu.A. Weiner, B.A. Gribkov, M.V. Zorina, A.E. Pestov, D.N. Rogachev, N.N. Salashchenko, N.I. Chkhalo. Izvestiya RAN. Seriya fizicheskaya, **75** (1), 71 (2011). (in Russian).
[19] S.S. Andreev, A.D. Akhsakhalyan, M.A. Bibishkin, N.N. Salashchenko, N.I. Chkhalo. Centr. Europ. J. Phys., **1**, 191 (2003).
[20] S.A. Garakhin, N.I. Chkhalo, I.A. Kas'kov, A.Ya. Lopatin, I.V. Malyshev, A.N. Nechay, A.E. Pestov, V.N. Polkovnikov, N.N. Salashchenko, M.V. Svechnikov, N.N. Tsybin, I.G. Zabrodin, S.Yu. Zuev. Rev. Sci. Instrum., **91** (6), 063103 (2020). https://doi.org/10.1063/1.5144489
[21] M. Suman, M.G. Pelizzo, D.L. Windt, G. Monaco, S. Zuccon, P. Nicolosi. Proc. SPIE, **19** (16), 14838 (2019).
[22] V.A. Slemzin, F.F. Goryaev, S.V. Kuzin. Plasma Phys. Reports, **40** (11), 855 (2014).
[23] A.J. Corso, M.G. Pelizzo. Proc. SPIE, 11116 (2019). DOI: 10.1117/12.2530208
[24] D.L. Windt. Comput. Phys., **12**, 360 (1998).